NACA

RESEARCH MEMORANDUM

INVESTIGATION OF MASS-FLOW AND PRESSURE-RECOVERY
CHARACTERISTICS OF SEVERAL UNDERSLUNG SCOOPTYPE INLETS AT FREE-STREAM MACH NUMBERS OF

2.0, 1.8, 1.5, AND 0.66

By Alfred S. Valerino and Robert F. Zappa

Lewis Flight Propulsion Laboratory Cleveland, Ohio

NATIONAL ADVISORY COMMITTEE FOR AERONAUTICS

WASHINGTON

March 13, 1957 Declassified March 18, 1960 Y

NATIONAL ADVISORY COMMITTEE FOR AERONAUTICS

RESEARCH MEMORANDUM

INVESTIGATION OF MASS-FLOW AND PRESSURE-RECOVERY CHARACTERISTICS

OF SEVERAL UNDERSLUNG SCOOP-TYPE INLETS AT FREE-STREAM

MACH NUMBERS OF 2.0, 1.8, 1.5, AND 0.66

By Alfred S. Valerino and Robert F. Zappa

SUMMARY

Several underslung scoop-type inlets mounted on a body of revolution were investigated at Mach numbers of 2.0, 1.8, 1.5, and 0.66 through an angle-of-attack range of -3° to 6°. Geometric differences between inlets included ramp angle, frontal area, splitter-plate height, and aspect ratio.

Some of the inlets investigated utilized auxiliary throat bleed. In general, throat bleed in conjunction with bypass flow increased the peak recoveries at Mach number of 2.0 throughout the angle-of-attack range. The best over-all angle-of-attack peak pressure recoveries were obtained with an inlet having a 10° precompression ramp ahead of the inlet. The stable subcritical range of all the inlets was practically nonexistent at a Mach number of 2.0. Severe pulsing was observed when the terminal shock was located slightly ahead of the splitter plate. Use of a flat plate projected into the path of the entering air delayed the onset of severe pulsing. Performance of one of the better inlets operating with design bypass flow was such that, if the inlet were matched with a turbojet engine, the total-pressure distortion would be essentially independent of Mach number and angle of attack.

TNTRODUCTION

Investigations of the performance of underslung scoop-type inlets have been conducted in the NACA Lewis 8- by 6-foot supersonic tunnel and are described in references 1 and 2. A continuation of these tests, utilizing the same basic model as reported in references 1 and 2 but employing other inlets, is reported herein.

Pressure-recovery and mass-flow characteristics of several inlets with boundary-layer removal ahead of the inlets were investigated at

free-stream Mach numbers of 2.0, 1.8, 1.5, and 0.66 and through an angle-of-attack range of -3° to 6°. Geometric differences between inlets investigated include ramp angle, frontal area, splitter-plate height, auxiliary throat bleed, and inlet aspect ratio. The peak-pressure-recovery characteristics of these inlets at angles of attack are compared with those of two inlets of reference 1.

SYMBOLS

A	area, sq ft
A	aspect ratio, ratio of inlet frontal height squared to frontal area
h	splitter-plate height
M	Mach number
m	mass flow
m_3/m_0	ratio of mass flow at compressor-face station to that in free-stream-tube area equal to inlet frontal area
P	total pressure
P _{3,max} - P _{3,min}	distortion .
W	inlet weight flow, lb/sec
$\frac{w_3\sqrt{\theta_3}}{\delta_3^1A_3}$	corrected weight flow at compressor face, (lb/sec)/sq ft
α	angle of attack, deg
δ	boundary-layer thickness
81	ratio of total pressure to NACA standard sea-level pressure of 2116 lb/sq ft
θ ,	ratio of total temperature to NACA standard sea-level temperature of 518.70 R
Subscripts:	

bypass

local
max maximum
min minimum

o free stream

inlet throat

compressor face

APPARATUS AND PROCEDURE

Apparatus

A schematic diagram of the model, which was a sting-mounted body of revolution with an underslung inlet, is presented in figure 1. Four sweptforward, single-oblique-shock inlets, designated as inlets 1 to 4, were investigated. Inlets 1, 3, and 4, as well as the approach C configuration of reference 1, had a flat approach ahead of the inlet (parallel to the model centerline). The approach B configuration of reference 1 had an approach angle of 1.28°, and inlet 2 had a 10°-precompression-ramp approach. Inlet 1 was also tested with a 10° precompression ramp ahead of the inlet.

Fuselage boundary-layer-removal systems were employed with each inlet. The boundary-layer air removed ahead of the inlets was either entirely diverted or partially taken aboard and then exhausted through ports on the side of the fuselage shown in figure 2.

Photographs and schematic diagrams of inlet configurations tested are presented in figures 3 and 4, respectively. Schematic diagrams of the inlets of reference 1 are given in figure 4(e). All the inlets were designed to operate at a Mach number of 2.0. The lips of the inlets were sweptforward at an angle of 43.75°, which approximates the oblique shock at design Mach number.

Variations in the geometry of the inlets and alterations to the inlets are listed in table I. As indicated, the inlets were sized to match three different engines (A, B, and C) requiring different airflows.

Area variations of inlets 1 to 4 are presented in figure 5. The local area is normal to the mean flow. Centerbodies simulating compressor hubs of turbojet engines were located in the forward position of a constantarea duct having a length of 43.4 inches. The nose of the centerbody extended into the diffuser. Mass flow through the inlet was remotely controlled by a plug located at the exit of the constant-area duct.

A slotted bleed ring, with slots along the duct periphery and alined with the main flow, was located upstream of the compressor-face station to bypass air that could be utilized for cooling or for an ejector-type exhaust nozzle. The bypass air, which was remotely controlled by means of a plug, was manifolded and then discharged axially through a 2-inch duct (shown in fig. 1). Test data were obtained at three bypass-plug positions: fully opened, closed, and a design setting predetermined from an earlier investigation of these inlets.

Instrumentation and Data Reduction

Instrumentation at the inlet throat station consisted of two total-pressure rakes to determine entrance total-pressure profiles. These rakes were removed as soon as entrance conditions were determined. At the compressor face, eight total-pressure rakes were installed and eight wall static taps were mounted on the centerbody. Total pressure at the compressor face was determined from an area-weighted average of the local total pressures. Total-pressure distortions were also obtained from the rake data.

At supersonic speeds, inlet mass flows were based on the average total pressure at the compressor face and a choked exit plug. Bypass mass flows were determined from four wall static orifices in the 2-inch constant-area duct and a choked exit plug. At free-stream Mach number of 0.66, however, neither the main nor the bypass exit plug was choked. Primary mass flows were based on average total and static pressures at the compressor face. Bypass mass flows were not obtainable at a Mach number of 0.66.

RESULTS AND DISCUSSION

Pressure-recovery and mass-flow characteristics of the inlets tested through an angle-of-attack range of -3° to 6° at Mach numbers of 2.0, 1.8, 1.5, and 0.66 are presented in figures 6 to 16.

Inlet Stability

At a Mach number of 2.0, with the exception of inlet l with the antibuzz plate (fig. 11), the subcritical stable range was very small. Schlieren observation indicated a fluttering of the lambda leg of the terminal shock when the shock approached the leading edge of the splitter plate. When the shock moved forward of the splitter plate, severe pulsing was noted. This is illustrated in the schlieren photographs shown in figure 17. As free-stream Mach number was decreased, the subcritical stable range increased. However, at the lower Mach numbers, the contraction ratio was too large to swallow the terminal shock.

Projection of the antibuzz plate into the path of the air entering inlet 1 considerably increased the subcritical stable range at all Mach numbers and angles of attack.

Peak Pressure Recoveries

The effects of angle of attack and inlet alterations on peak pressure recoveries are shown in figure 18. At free-stream Mach number of 2.0 (fig. 18(a)), bypassing low-energy air around the compressor did not significantly improve peak recoveries through the angle-of-attack range. The use of auxiliary throat bleed in conjunction with bypass air was effective in increasing the peak recovery at 0° angle of attack to approximately 84 percent (a 5-percent increase above that of inlet 1 with no bypass airflow). The throat-bleed configurations were sensitive to increases in angle of attack.

The best over-all angle-of-attack peak recoveries were obtained with inlet l utilizing the 10° precompression ramp. This inlet was relatively insensitive to increases in angle of attack. The effects of precompression are not clear in all cases, however, since the peak recoveries of inlet 2 with the 10° precompression ramp decreased with increasing angle of attack.

At Mach numbers of 1.8 and 1.5, there was essentially little difference in the angle-of-attack peak-recovery characteristics of the various inlets investigated.

The peak recoveries of these inlets are compared with those of the inlet configurations of reference 1 in figure 18(b). At Mach 2.0, the approach B configuration of reference 1 and inlet 2 with auxiliary throat bleed had comparable performance, while the approach C configuration of reference 1 was comparable to inlet 2 without throat bleed.

Total-Pressure Distortions

Typical total-pressure distortions at the compressor face of inlet 1 with and without auxiliary throat bleed are presented in figure 19. Use of throat bleed with bypass flow did not reduce the distortion level; the distortions were essentially the same as those of inlet 1 with design bypass flow. Increases in bypass flow increased the distortion level.

With inlet 1 operating with design bypass flow and matched to turbojet engine A, requiring corrected weight flows at the compressor face of approximately 28, 31, and 35 pounds per second at free-stream Mach numNACA RM E56K29

bers of 2.0, 1.8, and 1.5, respectively, the magnitude of distortion was independent of Mach number and angle of attack (distortion magnitude of 15 to 18 percent).

Typical total-pressure-contour maps of inlet 1 with and without auxiliary throat bleed and with the 10° precompression ramp are presented in figures 20 to 22. At Mach numbers of 1.5, 1.8, and 2.0, use of throat bleed with design bypass flow did not significantly affect the location of the high-pressure areas. In general, the high-pressure lobes either surrounded the centerbody or were found in the lower central portion of the duct.

Use of precompression ahead of inlet 1 at Mach numbers of 1.5 and 1.8 did not significantly affect the high-pressure-lobe location. At Mach 2.0, precompression shifted the duct high-pressure area in a manner which varied with inlet operating conditions.

Typical total-pressure profiles at the throats of inlet 1 and 2 are similar, as shown in figure 23. However, the total pressures near the top of the duct (approx. 3 in. from inlet floor) were slightly higher in inlet 2 because of the precompression surface ahead of the inlet.

SUMMARY OF RESULTS

A series of underslung scoop-type inlets, with and without auxiliary throat bleed, were investigated through an angle-of-attack range of -3° to 6° and at Mach numbers of 0.66, 1.5, 1.8, and 2.0. Geometric differences between inlets included ramp angle, frontal area, splitter-plate height, and inlet aspect ratio. The following results were obtained:

- 1. In general, use of throat bleed in conjunction with bypass flow resulted in increases in peak pressure recoveries throughout the angle-of-attack range at a free-stream Mach number of 2.0.
- 2. Best over-all angle-of-attack peak recoveries were obtained with inlet 1 employing a 10° precompression ramp ahead of the inlet; the inlet was relatively insensitive to angle of attack.
- 3. Stable subcritical operation of the inlet configurations was practically nonexistent at a free-stream Mach number of 2.0. Severe pulsing occurred when the terminal shock was positioned slightly ahead of the splitter plate.
- 4. The projection of a flat plate into the path of the entering air delayed the onset of severe pulsing.

NACA RM E56K29

5. For a turbojet engine matched to inlet 1 operating with design bypass flow, the total-pressure-distortion level was essentially independent of Mach number and angle of attack.

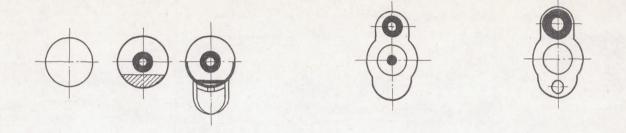
Lewis Flight Propulsion Laboratory
National Advisory Committee for Aeronautics
Cleveland, Ohio, December 18, 1956

REFERENCES

- 1. Weinstein, Maynard I., Vargo, Donald J., and McKevitt, Frank: Investigation of an Underslung Scoop Inlet at Mach Numbers to 1.99.
 NACA RM E56L11, 1957.
- 2. Vargo, Donald J., and Weinstein, Maynard I.: Investigation of an Underslung Normal-Wedge Inlet at Free-Stream Mach Numbers from 1.50 to 1.99. NACA RM E56F27, 1957.

TABLE I. - INLET GEOMETRY AND ALTERATIONS

Inlet	Engine	Ramp angle, deg	Frontal area, sq ft	Aspect ratio,	Splitter- plate height, h, in.	h/δ at $M_0 = 2.0$, $\alpha = 0^{\circ}$	Alterations
1 A	A	14	0.174	0.78	0.543	0.776	(a) Flush throat slot having area equal to 0.15 throat area
						0.776	(b) Ram throat slot having height equal to 0.17 in., area = 0.10 throat area
				* * * * * * * * * * * * * * * * * * *		0.776	(c) Reduced throat slot having area equal to 0.15 throat area
				5* 			(d) 10° Precompression ramp forward of inlet
	1				0.776	(e) 1.423- by 1.613-in. flat anti- buzz plate at station 82.15	
2	В	12	0.141	0.79	0.406		(a) 10° Precompression ramp (b) 10° Precompression ramp with flush throat slot having area equal to 0.12 throat area
3	C	14	0.154	0.71	0.543	0.776	None
4	В	12	0.143	0.62	0.543	0.776	None
Reference 1, approach C (short splitter)	В	14.2	0.131	0.99	0.68	1.2	
Reference 1, approach B (flush ceil- ing slot)	В	14.2	0.131	0.99	0.39	0.68	



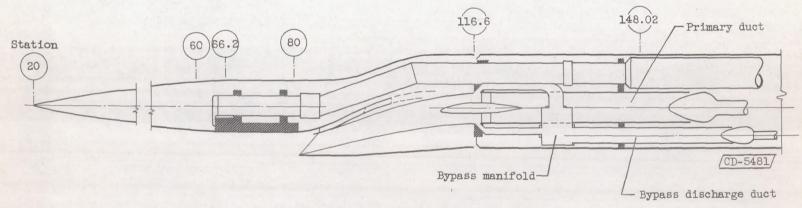


Figure 1. - Schematic diagram of model.

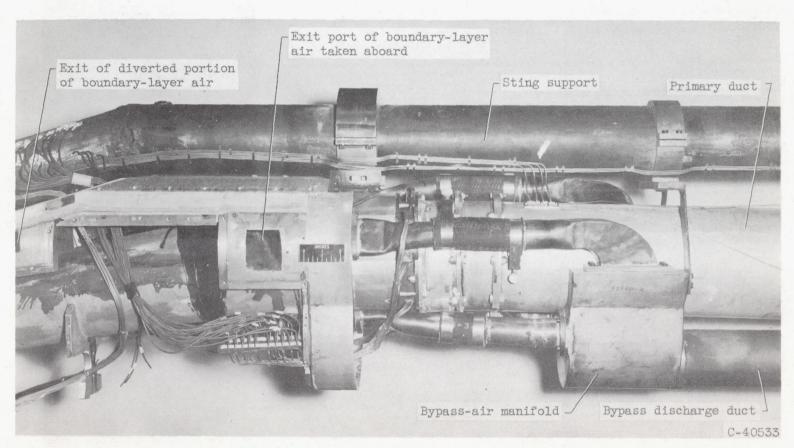
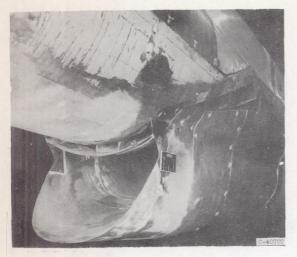
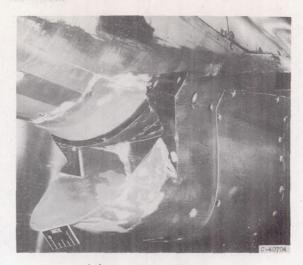


Figure 2. - Model assembly.

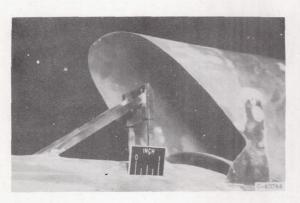
NACA RM E56K29



(a) Inlet 1 with reduced throat slot.



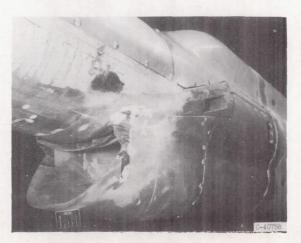
(b) Inlet 1 with precompression ramp.



(c) Inlet 1 with antibuzz plate.



(d) Inlet 2.



(e) Inlet 3.

Figure 3. - Photographs of inlet configurations.

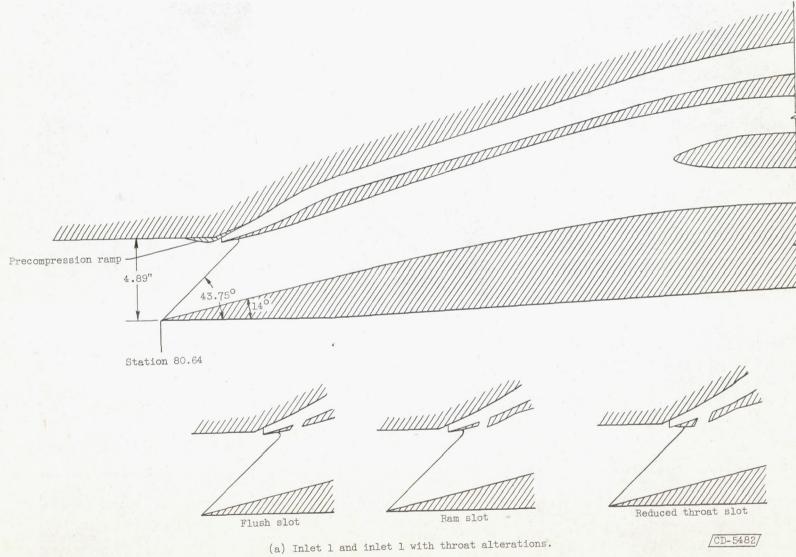
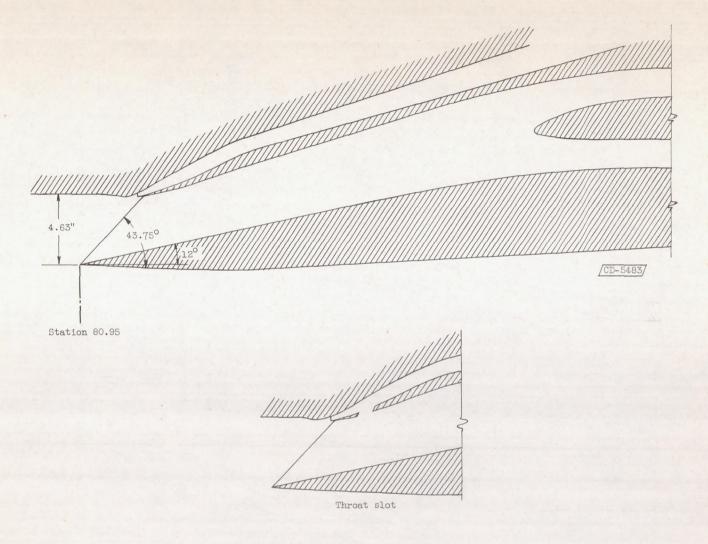


Figure 4. - Schematic diagrams of inlet configurations.



(b) Inlet 2 and inlet 2 with throat alteration.

Figure 4. - Continued. Schematic diagrams of inlet configurations.

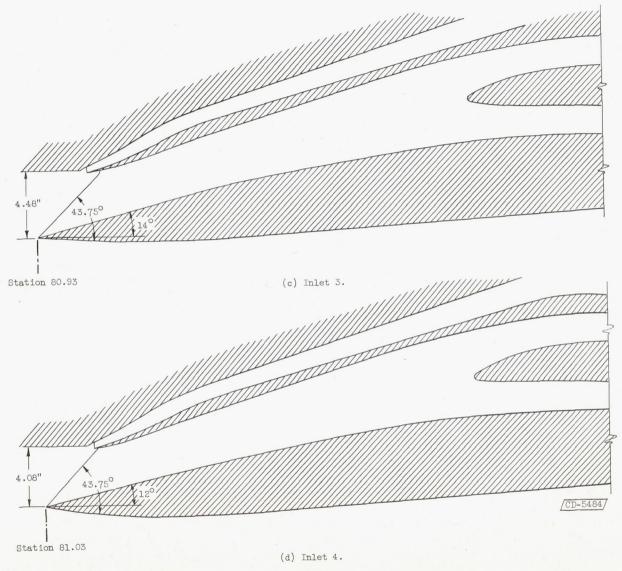
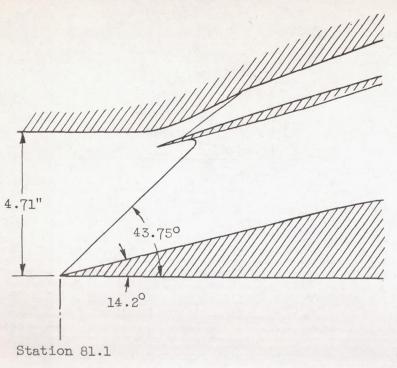


Figure 4. - Continued. Schematic diagrams of inlet configurations.

CD-5485/



Approach C (short splitter)

Approach B (flush ceiling slot)

5.00"

1.28°

43.750

14.20

(e) Inlet configurations of reference 1.

Figure 4. - Concluded. Schematic diagrams of inlet configurations.

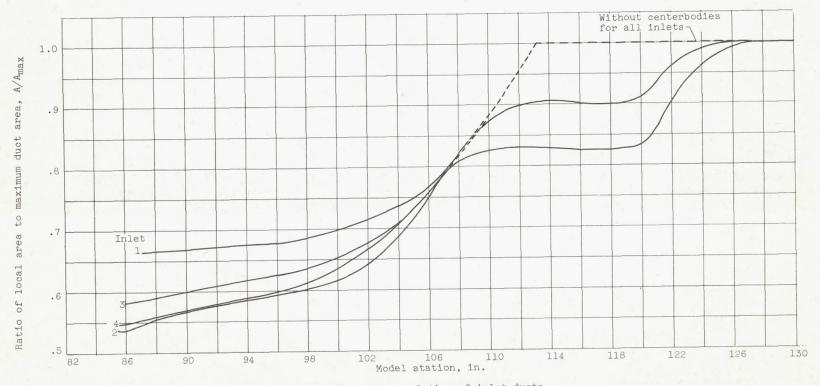


Figure 5. - Area variation of inlet ducts.

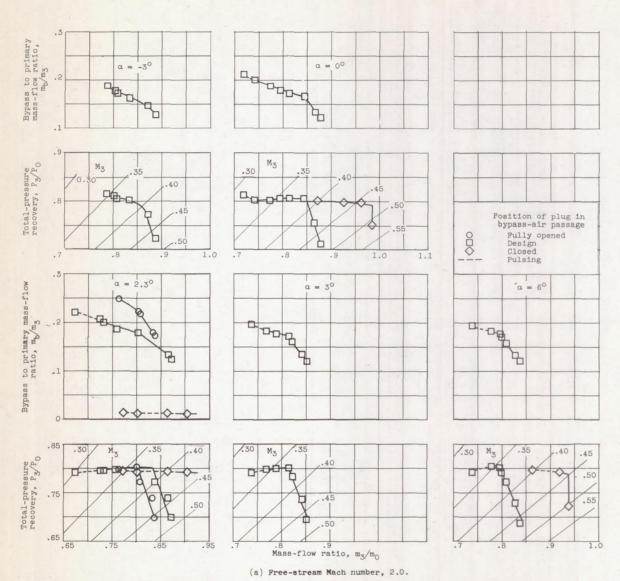


Figure 6. - Effect of bypass flow on pressure-recovery and mass-flow characteristics of inlet 1 with no auxiliary throat bleed.

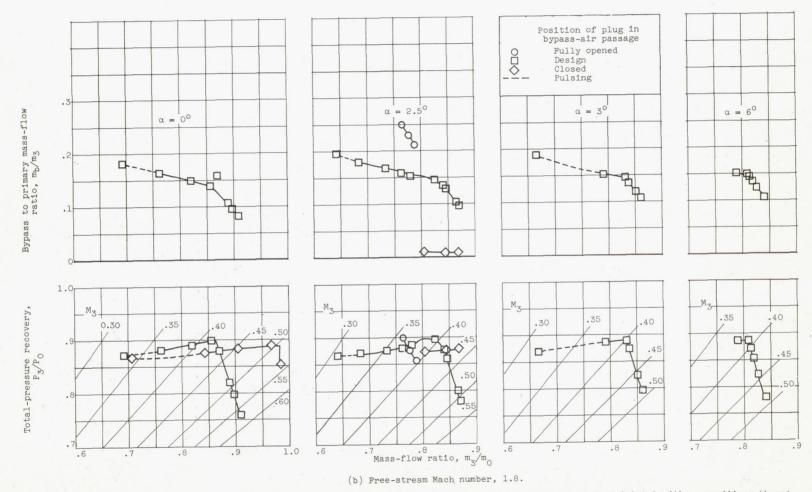


Figure 6. - Continued. Effect of bypass flow on pressure-recovery and mass-flow characteristics of inlet 1 with no auxiliary throat bleed.

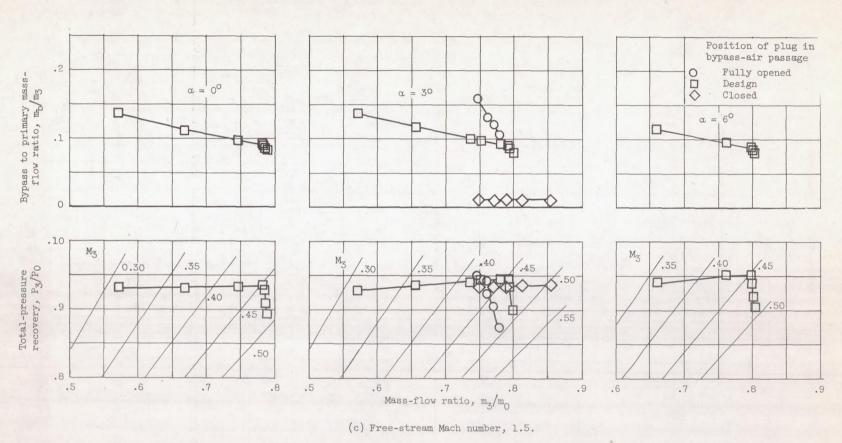
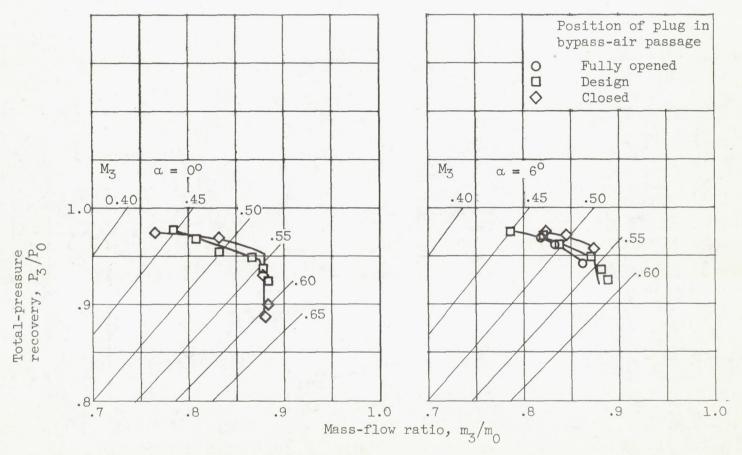


Figure 6. - Continued. Effect of bypass flow on pressure-recovery and mass-flow characteristics of inlet 1 with no auxiliary throat bleed.



(d) Free-stream Mach number, 0.66.

Figure 6. - Concluded. Effect of bypass flow on pressure-recovery and mass-flow characteristics of inlet 1 with no auxiliary throat bleed.

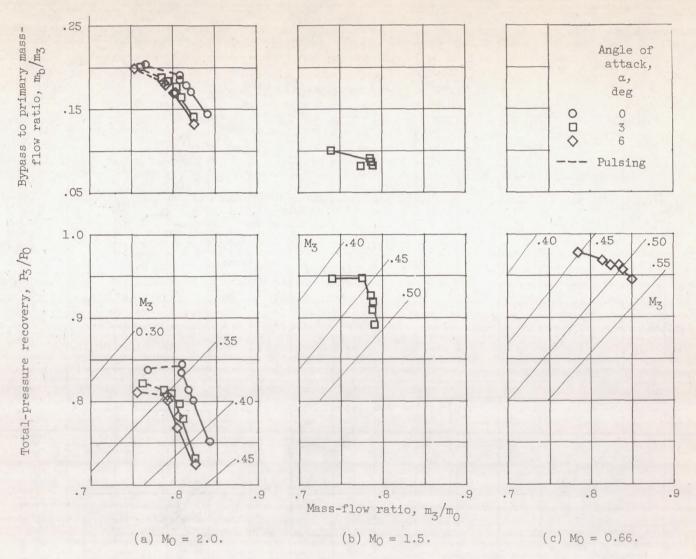


Figure 7. - Pressure-recovery and mass-flow characteristics of inlet 1 with flush throat slot. Design bypass-plug position.

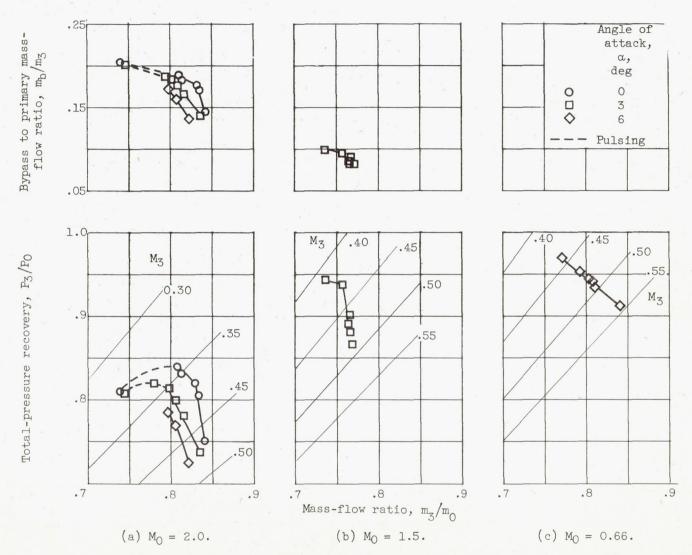


Figure 8. - Pressure-recovery and mass-flow characteristics of inlet 1 with ram throat slot. Design bypass-plug position.

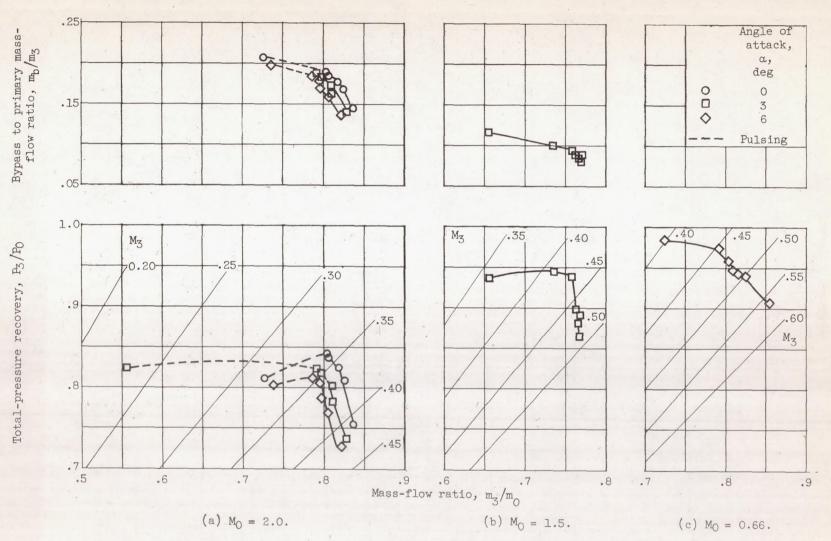


Figure 9. - Pressure-recovery and mass-flow characteristics of inlet 1 with reduced throat slot. Design bypass-plug position.

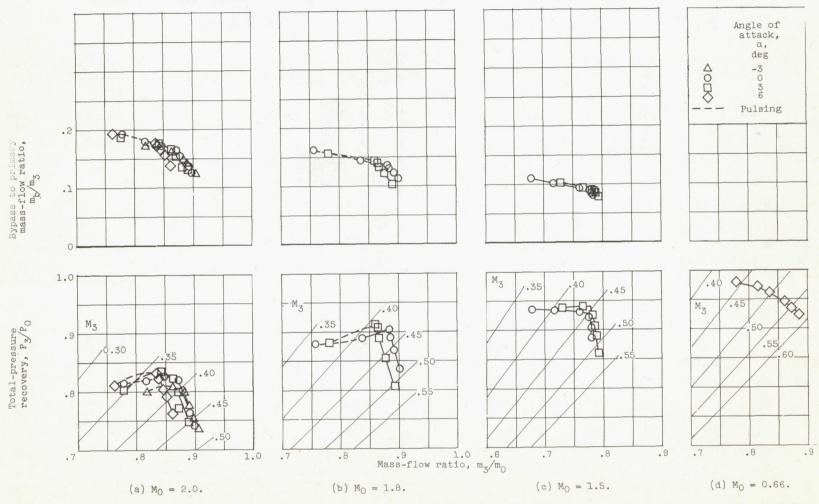


Figure 10. - Pressure-recovery and mass-flow characteristics of inlet 1 with precompression ramp. Design bypass-plug position.

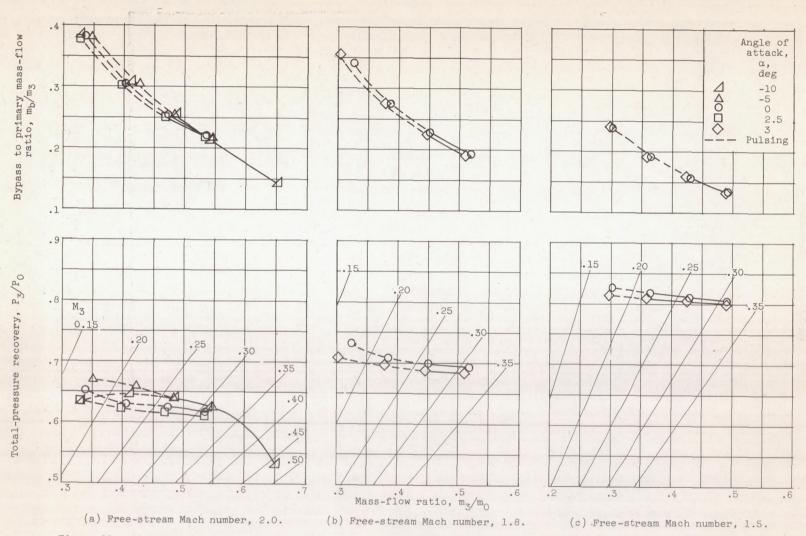


Figure 11. - Pressure-recovery and mass-flow characteristics of inlet 1 with antibuzz plate. Design bypass-plug position.

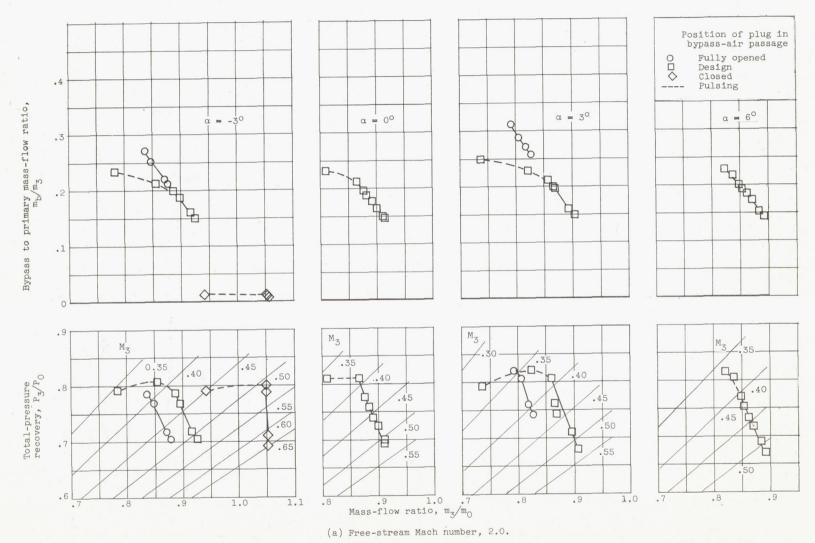


Figure 12. - Effect of bypass flow on pressure-recovery and mass-flow characteristics of inlet 2 with no auxiliary throat bleed.

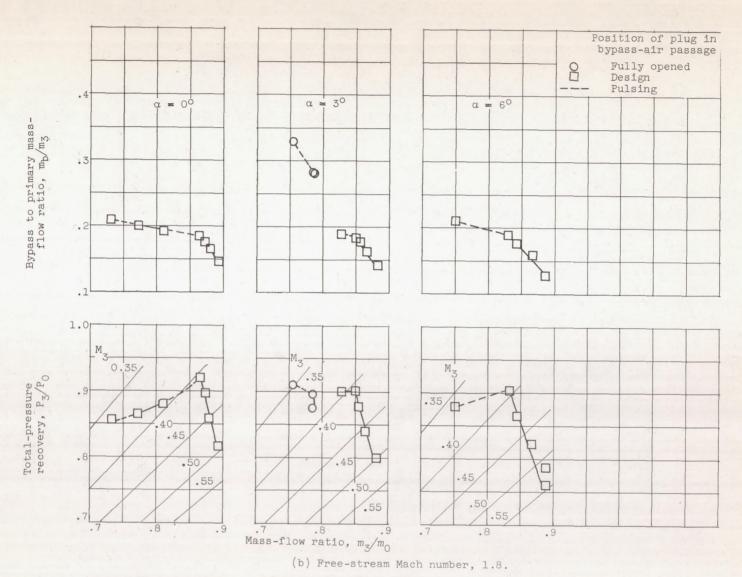
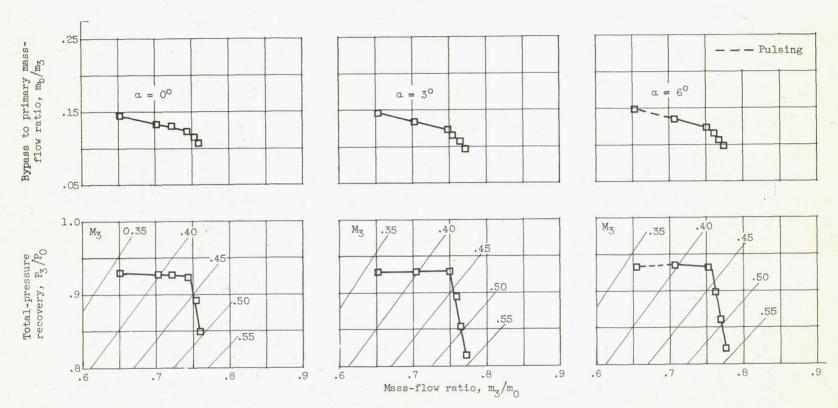


Figure 12. - Continued. Effect of bypass flow on pressure-recovery and mass-flow characteristics of inlet 2 with no auxiliary throat bleed.



(c) Free-stream Mach number, 1.5. Design bypass-plug position.

Figure 12. - Concluded. Effect of bypass flow on pressure-recovery and mass-flow characteristics of inlet 2 with no auxiliary throat bleed.

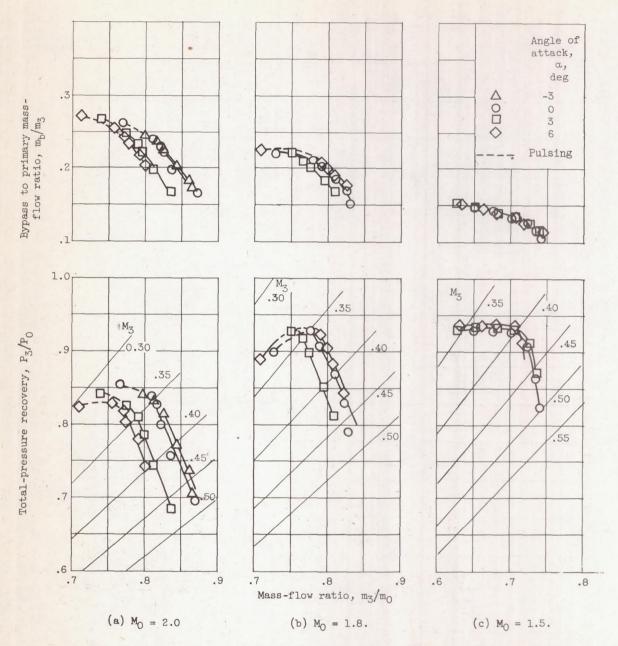


Figure 13. - Pressure-recovery and mass-flow characteristics of inlet 2 with flush throat slot. Design bypass-plug position.

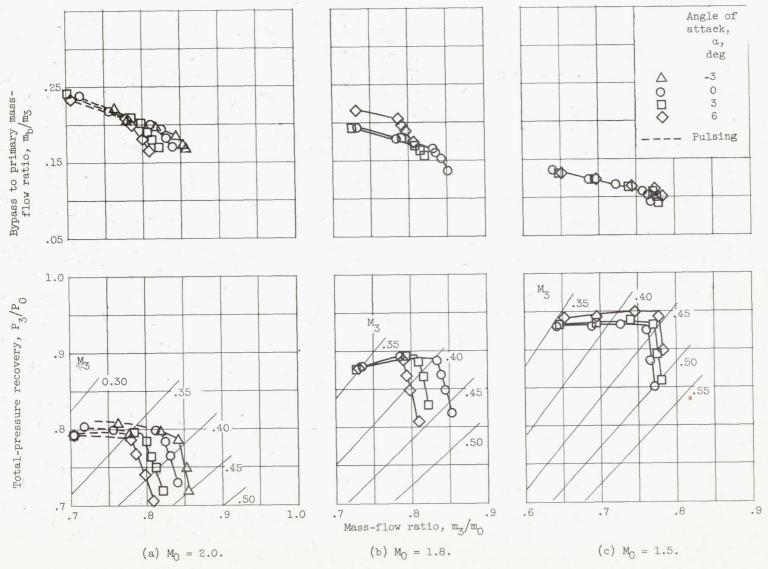


Figure 14. - Pressure-recovery and mass-flow characteristics of inlet 3. Design bypass-plug position.

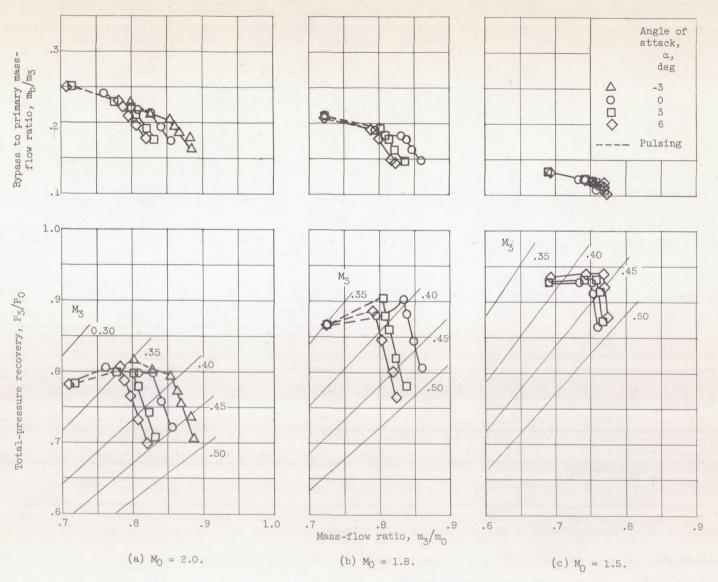


Figure 15. - Pressure-recovery and mass-flow characteristics of inlet 4. Design bypass-plug position.

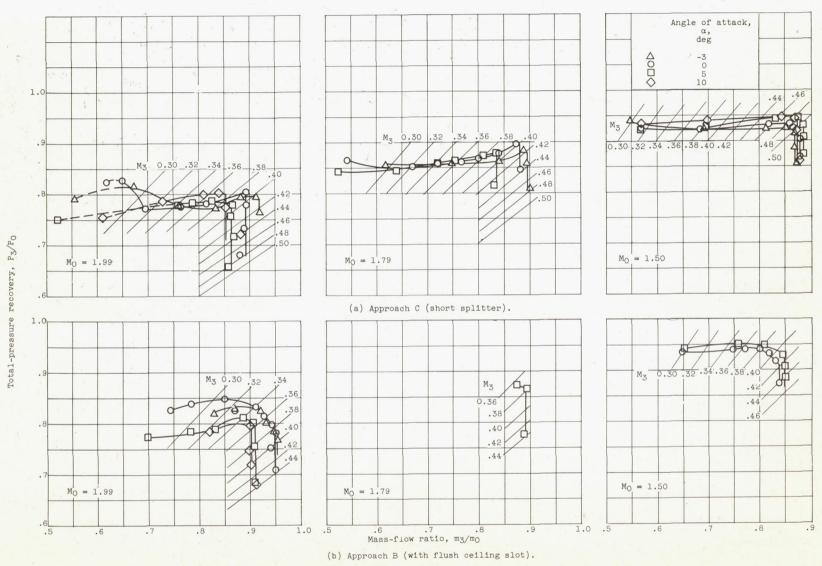


Figure 16. - Pressure-recovery and mass-flow characteristics of inlet configurations of reference 1. Zero bypass flow.

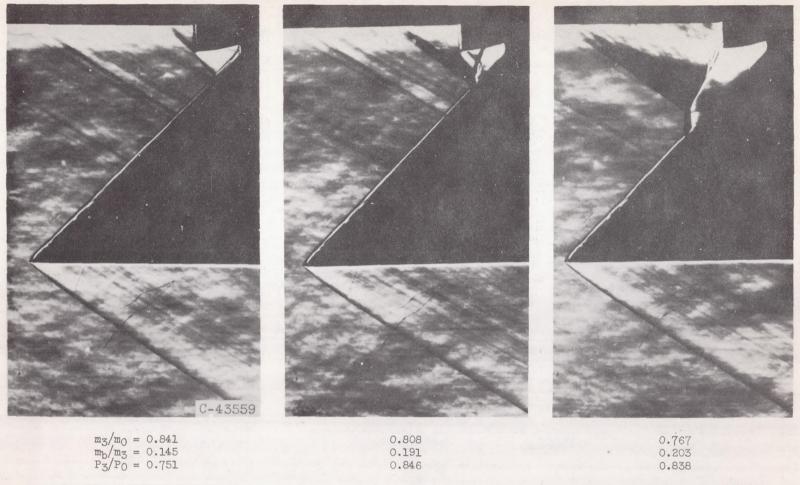


Figure 17. - Schlieren photographs of inlet 1 with flush throat slot at free-stream Mach number of 2.0 and 0° angle of attack.

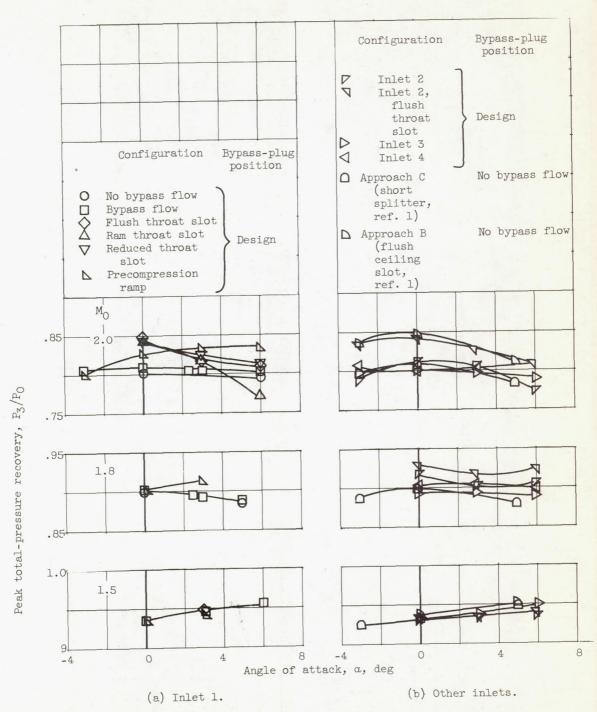


Figure 18. - Effects of angle of attack and inlet alterations on peak pressure recoveries of inlets.

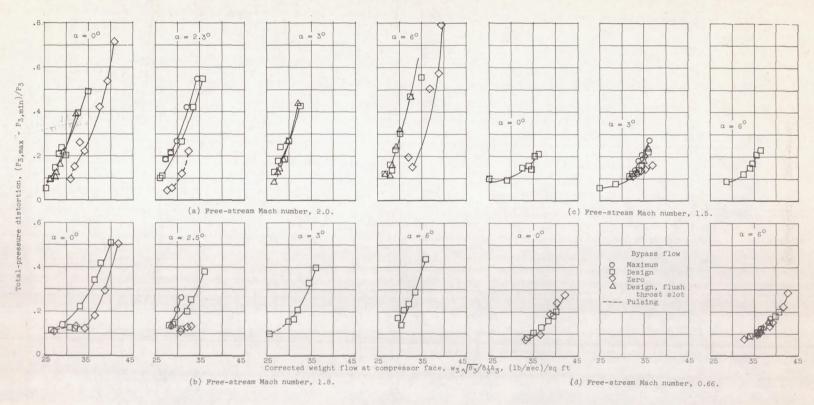


Figure 19. - Typical total-pressure distortions at compressor face for inlet 1.

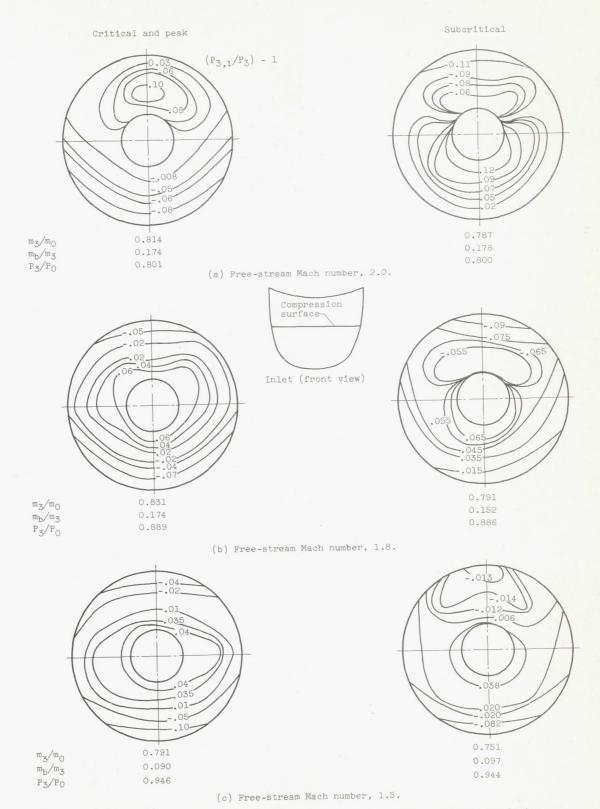


Figure 20. - Total-pressure contours at compressor-face station of inlet 1. Design bypass-plug position; angle of attack, 3° .

37

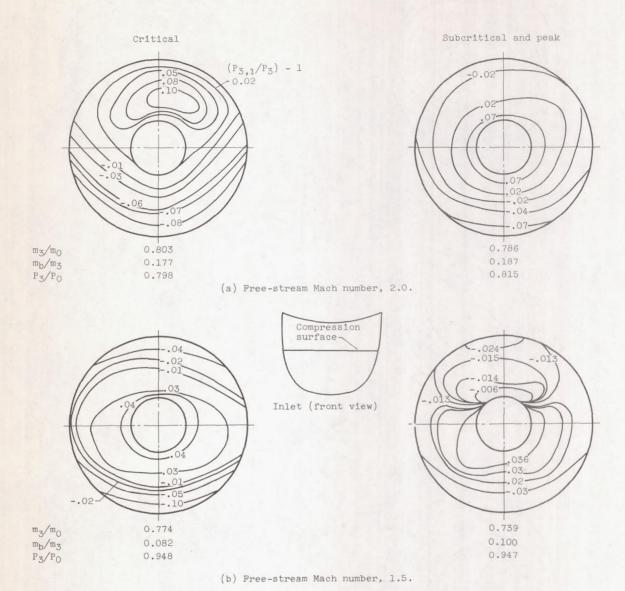


Figure 21. - Total-pressure contours at compressor-face station of inlet 1 with flush throat slot. Design bypass-plug position; angle of attack, 30.

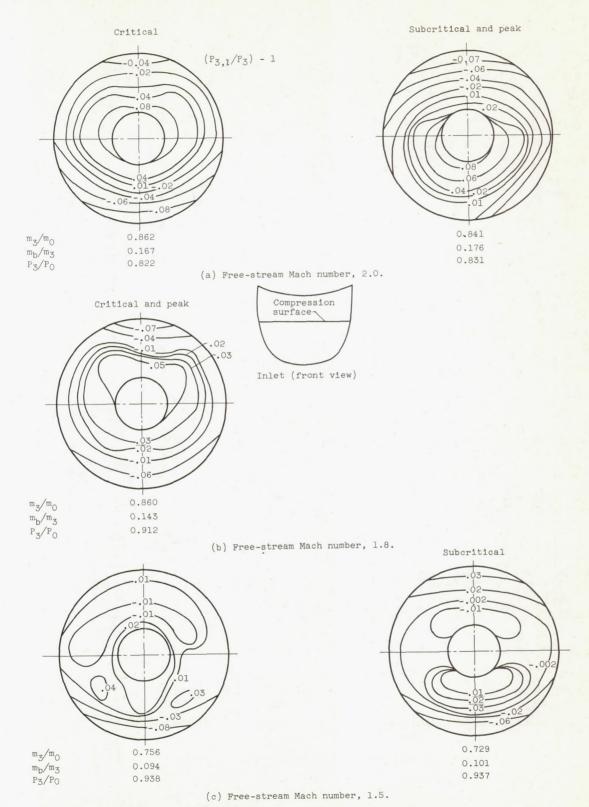


Figure 22. - Total-pressure contours at compressor-face station of inlet 1 with precompression ramp. Design bypass-plug position; angle of attack, 3°.

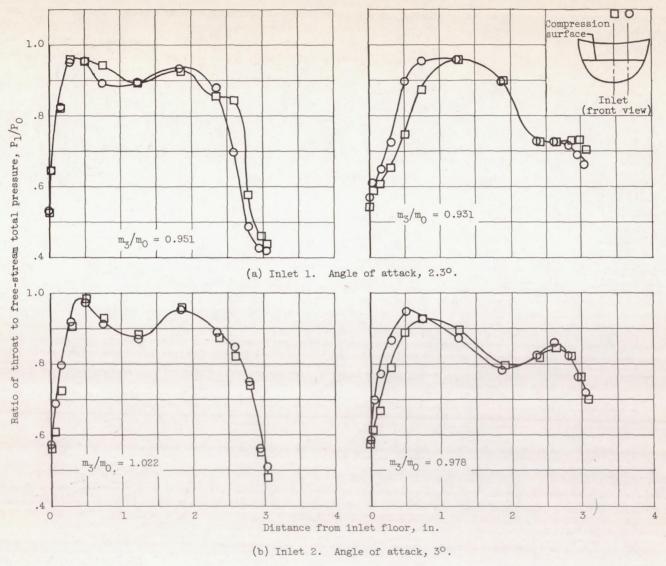


Figure 23. - Typical throat total-pressure profiles of inlets 1 and 2. Free-stream Mach number, 2.0.